68º congresso anual da abm
68th abm international annual congress
ISSN 1516-392X

COMPLIANCE SOLUTIONS INCLUDING 3-D AND SIDE-GROOVE EFFECTS APPLICABLE TO CRACK SIZE ESTIMATION USING C(T), SE(B) AND CLAMPED SE(T) SPECIMENS[1]

Felipe Cavalheiro Moreira[2]
Gustavo Henrique Bolognesi Donato[3]

Abstract
Experiments regarding J-resistance curves and fatigue crack growth usually employ elastic compliance (C) techniques to estimate instantaneous crack size (a). This estimation derives from C using a dimensionless parameter (μ) which incorporates specimen's thickness (B), elasticity (E) and compliance itself. Plane stress and plane strain solutions for μ are available: the work of Tada et al. from 1985, ASTM-E1820 and ASTM-E647 provide solutions for C(T), SE(B) and M(T) specimens, among others. Current challenges include: i) real specimens are in neither plane stress nor plane strain - modulus vary between E (plane stress) and $E/(1-\nu^2)$ (plane strain); ii) furthermore, the existence of side-grooves affect specimen's stiffness, leading to an "effective thickness" with deviations larger than 10% in crack size estimations following current practices, especially for shallow-cracked samples. As a step in this direction, this work investigates 3-D and side-groove effects on compliance solutions applicable to C(T), SE(B) and SE(T) specimens. Refined 3-D elastic FE-models provide Load-CMOD evolutions. Crack depths between a/W=0.1 and a/W=0.7 on 1/2T, 1T and 2T geometries with width to thickness ratio W/B=2 are investigated. Side-grooves of 5%, 10% and 20% are considered. The results include compliance solutions incorporating 3D and side-groove effects to provide accurate crack size estimation during laboratory fracture and FCG testing. The proposals were verified against current standardized solutions and deviations were strongly reduced.
Key words: Compliance solutions; 3D effects; Side-groove; Fracture specimens.

[1] *Technical contribution to 68th ABM International Congress, July, 30th to August 2nd, 2012, Belo Horizonte, MG, Brazil*
[2] *Mechanical Engineer, Master student, Mechanical Engineering Department, FEI, São Bernardo do Campo, Brazil; femoreira@fei.edu.br.*
[3] *Mechanical Engineer, D.Sc., Professor, Mechanical Engineering Department, FEI, São Bernardo do Campo, Brazil; gdonato@fei.edu.br.*

ISSN 1516-392X

1 INTRODUCTION

Conventional procedures for design and integrity assessment of structural components containing crack-like defects are based on fracture mechanics theory and rely upon the notion that a single parameter which defines the crack driving force characterizes the fracture resistance of the material.[1] This is of particular relevance for real applications in which structures are assessed against fracture (in terms of K or J integral) or fatigue crack growth (in terms da/dN *vs.* ΔK or ΔJ). Several recommended practices can be found, for example, in API RP 579,[2] BS 7910,[3] R6,[4] SINTAP[5] or DNV-OS-F101[6] and will not be addressed here due to space limitations. However, to properly support these structural integrity evaluations regarding safety and lifetime predictions, accurate mechanical properties including fracture toughness and fatigue crack growth (FCG) data is mandatory and motivates this investigation.

In the case of fracture phenomena in current high-toughness structural steels (for example applicable to pipelines, pressure vessels and other pressurized components), assessment usually demands the theoretical background of Elastic-Plastic Fracture Mechanics (EPFM). In terms of crack-driving forces, the elastic-plastic macroscopic loading can be characterized by J integral or the (analogous) Crack Tip Opening Displacement (CTOD, δ). If the material experiences unstable fracture (e.g. cleavage in ferritic steels), toughness can be described in terms of critical parameters (J_c or δ_c).[1] Conversely, if severe plasticity takes place and ductile tearing occurs, resistance against ductile crack propagation is usually evaluated based on crack growing curves (usually referred to as R-curves[1]). Depending on the crack-driving force considered for the computations, R-curves can be denoted J-R or δ-R, and they are of paramount relevance nowadays since most structural materials present high toughness and cannot be characterized by J_c or δ_c. The basis of R-curves is to quantify crack extension (Δa) caused by applied J or δ levels and therefore real-time estimation of accurate crack size is mandatory. Considering the interests of this study, the most complete and relevant standardized procedures for fracture resistance evaluation are ASTM E1820,[7] ISO 12135[8] and DNV-RP-F108.[9] Those three standards represent unified methods for determining fracture toughness in terms of K, δ, J and (excluding the latter procedure) R-curves for homogeneous metallic materials subjected to quasistatic loading. In most cases only C(T) and SE(B) specimens are covered. Figures 1a and 1b presents the corresponding geometrical features, but additional requirements will be detailed and addressed later.

In view of interest from the chemical and petroleum industry regarding safety and performance of pipeline systems and pressurized components, clamped SE(T) specimens loaded under tension will also be considered for this study (Figure 1c). As previously shown by Moreira and Donato[1010] and Cravero and Ruggieri,[11] this configuration presents much better description of pressurized pipelines and pressure vessels crack-tip stress fields than conventional C(T) or SE(B) specimens. From the aforementioned standards, only DNV-RP-F108[9] accommodates SE(T) specimens, but provides solutions restricted to J and δ estimation. Compliance solutions for crack size estimation are not available and R-curves cannot be formally estimated. Some solutions for SE(T) specimens can be found in Cravero and Ruggieri[12] and will serve as a reference here.

In the case of fatigue crack growth (FCG) testing, the most widespread standard is ASTM E647.[13] As will be detailed next in section 3, FCG data is usually

ISSN 1516-392X

characterized by the crack growth rate *da/dN* caused by a cyclic loading applied to a cracked component and which leads to a range of crack-driving force *ΔK* (assuming Linear-Elastic Fracture Mechanics). Once again, the accurate estimation of crack size during laboratory test is essential to provide accurate crack growth rates. This procedure covers C(T), middle tension M(T) and eccentrically-loaded single edge crack tension ESE(T) specimens, but only C(T) is of practical interest for this study.
Results presented by Shen, Thyson and Gianetto in 2010[14] and 2012[15] and tests conducted by current authors revealed deviations larger than 10% in crack size estimations following available practices, especially for shallow-cracked specimens containing side-grooves. As a step to increase accuracy in crack size estimation using unloading compliance technique, this work investigates 3-D and side-groove effects on compliance solutions applicable to C(T), SE(B) and clamped SE(T) specimens. Refined 3-D elastic FE-models provide Load-CMOD evolutions. The analysis matrix includes crack relative depths between $a/W=0.1$ and $a/W=0.7$ on *1/2T*, *1T* and *2T* geometries. The *1T* geometry is taken as the reference and presents width to thickness ratio $W/B=2$. Side-grooves of 5%, 10% and 20% are considered. A special mesh generator was developed and very refined mesh pattern could be guaranteed. The results include effective thicknesses and compliance solutions incorporating 3D and side-groove effects for C(T), SE(B) and clamped SE(T) specimens.

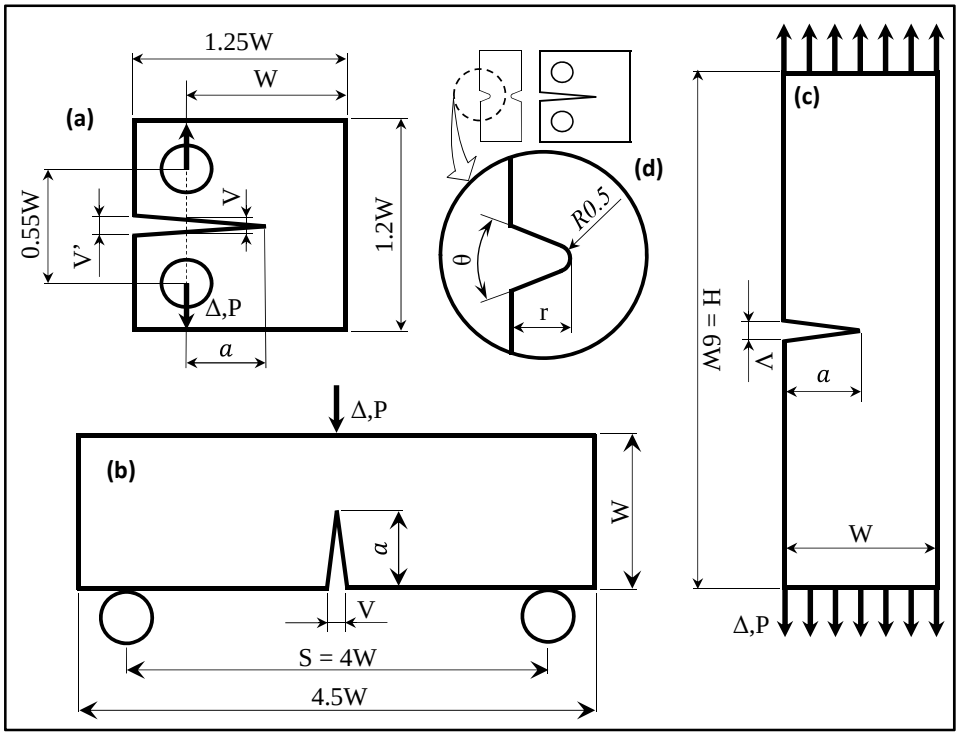

Figure 1. Fracture specimens: (a) compact tension C(T), (b) single-edge notched under bending SE(B) and (c) clamped single-edge notched under tension SE(T). (d) Geometrical features of side-grooves following ASTM E1820.[7] *P* denotes applied load, *V* the Crack Mouth Opening Displacement (*CMOD*) and *Δ* the Load-Line Displacement (*LLD*). Thickness *B* = 25.4 mm for 1T specimens.

ISSN 1516-392X

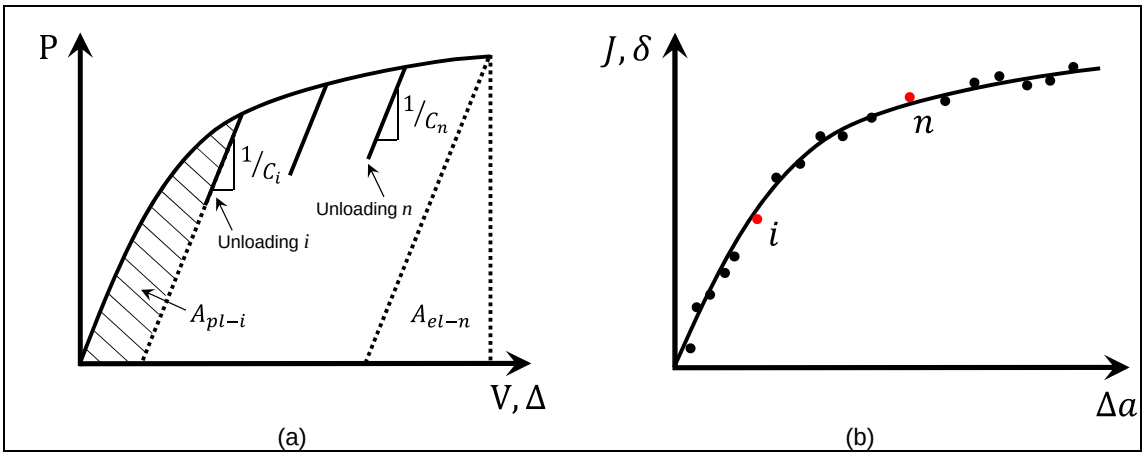

Figure 2. (a) Load-displacement curve including partial unloadings and different compliances *C* and (b) schematic *R*-curve relating *J* or *δ* to crack extension *Δa*.

2 *R-CURVE* TESTING

*R-curve*s (Figure 2b) quantify the relationship between applied crack-driving force (J or δ) and crack extension (Δa) and are of great relevance to characterize materials that exhibit stable tearing. Laboratory testing can be conducted based on single-specimen or multi-specimen techniques.[1] The first option is time consuming and economically onerous and single-specimen techniques are preferred nowadays.
The most common single-specimen technique is the unloading compliance method, which is illustrated in Figure 2a. The specimen is monotonically loaded and partially unloaded several times during crack extension. Load (P) is recorded *vs.* displacement (in terms of CMOD – V or LLD - Δ) during the whole test (in this work, V will be used). Elastic and plastic areas (respectively A_{pl} and A_{el}) are the basis for calculating instantaneous crack-driving forces and details can be found, for example, in ASTM E1820[7] using the eta (η) method. In each unloading, the stiffness ($1/C$) can be computed based on P-V data and reflects crack size at that moment. Testing standards provide polynomial expressions that relate instantaneous a/W to the experimental compliance C. Considering two unloadings "*i*" and "*n*" applied to the same specimen as illustrated in Figure 2a, the respective J-Δa points in Figure 2b can be obtained. Further details can be found in the work of Saxena,[16] but the need for accurate expressions to correlate a/W to compliance is clear.

3 FATIGUE CRACK GROWTH (FCG) TESTING

Fatigue crack growth testing also employs fracture mechanics specimens (in most cases C(T) geometry), but looking for the material's resistance against crack propagation under cyclic loading. Further details can be found in Anderson[1] and Suresh[17] and in ASTM E647,[13] but in simple terms a specimen is tested under load control (fixed P) during thousands of cycles, usually with loading ratio ($R = P_{min}/P_{max}$) larger than zero to minimize closure and residual stress effects[17]. During the test the crack grows and the stress intensity factor range (ΔK) or J integral range (ΔJ) increases, which is illustrated in Figure 3a. At the moment "*i*", the crack size is a_i and it means a stiffness $1/C_i$. At the moment "*n*", $a_n > a_i$ and the specimen presents lower stiffness $1/C_n$. Based on applied ΔK or ΔJ and respective compliances, instantaneous crack size can be computed and da/dN *vs.* ΔK or da/dN *vs.* ΔJ evolutions determined (Figure 3b). These trajectories represent the basis for life prediction considering

ISSN 1516-392X

fatigue crack growth phenomenon. Similarly to *R*-curve testing, it can be noted that FCG experiments are highly dependent on accurate expressions that relate instantaneous a/W to the experimental compliance C.

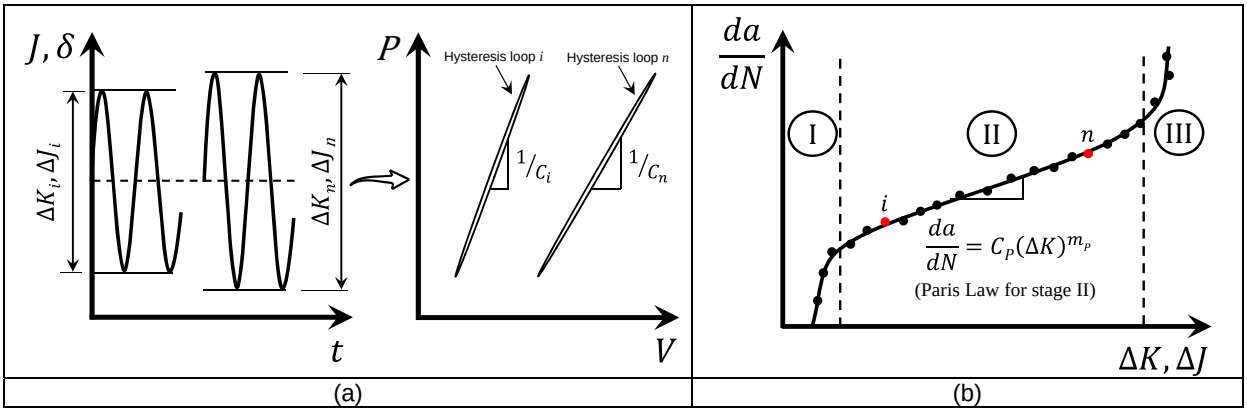

Figure 3. (a) Cyclic loading under load control (fixed P) leading to fatigue crack growth and therefore increasing ΔK, ΔJ and C. (b) Schematic FCG response including the well-known Paris law for stage II.

4 REVISION OF AVAILABLE SOLUTIONS FOR CRACK-SIZE ESTIMATION USING THE UNLOADING COMPLIANCE METHOD

Several studies regarding elastic compliance solutions for fracture mechanics specimens are available. Some of them are based on solid mechanics analytical evaluations and others are based on refined FEM computations. Most solutions are based on FEM computations using plane strain or plane stress models, without considering 3D or side-groove effects, being a renowned reference the work of Tada, Paris and Irwin.[18] For practical purposes, the standards and references considered by the authors as being the most accurate to the present date are presented next.
Considering C(T) specimens and *P*-*V* records measured aligned to the load line (Figure 1a), ASTM E1820[7] and ASTM E647[13] estimate a/W in the form

$$a/W = 1.000196 - 4.06319\,\mu + 11.242\,\mu^2 - 106.043\,\mu^3 + 464.335\,\mu^4 - 650.677\,\mu^5 \quad (0.200 \le a/W \le 0.975) \quad (1)$$

where the normalized elastic compliance (μ) is given by

$$\mu = \frac{1}{\sqrt{B_{eff}\,EC} + 1} \quad (2)$$

The elastic compliance ($C = \Delta V/\Delta P$) is obtained for each unloading (for *R*-curve testing) or hysteresis loop (for FCG testing) as presented by sections 2 and 3 (Figures 2a and 3a). The effective thickness (B_{eff}) accounts for side-groove effects and can be computed as

$$B_{eff} = B - \frac{(B - B_N)^2}{B}, \quad (3)$$

where B_N is the net thickness ($B_N = B\text{-}2r$ - Figure 1d). Corrections for specimen rotation or CMOD (V) measured in different locations (away from the load line) are available in the same standards and should be taken into account.
Solutions for SE(B) specimens are also available in 2011 version of ASTM E1820[7] based on a work of Joyce[19] (Equation 4) for shallow cracks and on a work of Wu[20] (Equation 5) for deep cracks. Alternative formulae can be found on a recent review

ISSN 1516-392X

conducted by Wang and Zhou,[21] but Joyce's and Wu's results are the most accurate.

$$a/W = 1.01878 - 4.5367\,\mu + 9.0101\,\mu^2 - 27.333\,\mu^3 + 74.400\,\mu^4 - 71.489\,\mu^5 \quad (0.050 \le a/W \le 0.450) \tag{4}$$

$$a/W = 0.999748 - 3.9504\,\mu + 2.9821\,\mu^2 - 3.21408\,\mu^3 + 51.51564\,\mu^4 - 113.031\,\mu^5 \quad (0.300 \le a/W \le 1.000) \tag{5}$$

In Equations 4 and 5, B_{eff} comes from Equation 3 and the normalized compliance (μ)

$$\mu = \frac{1}{\sqrt{\frac{B_{eff} WEC}{S/4}} + 1} \,. \tag{6}$$

Clamped SE(T) specimens, in its turn, are only supported by DNV-RP-F108,[9] but available solutions are restricted to J and δ estimation. Compliance solutions are not included. However, some results presented by Cravero and Ruggieri[12] will serve as a basis for this investigation and follow. Considering $H = 6W$, this reference suggests that a/W can be estimated using unloading compliance in the form

$$a/W = 2.1263 - 13.461\,\mu + 51.299\,\mu^2 - 120.47\,\mu^3 + 147.83\,\mu^4 - 71.812\,\mu^5 \quad (0.100 \le a/W \le 0.70) \tag{7}$$

where the normalized elastic compliance (μ) is given by Equation 2 similarly to C(T) geometry. For clamped SE(T) specimens, Equation 7 is sensitive to the relative length of the specimen (H/W – Figure 1c), particularly for $a/W \ge 0.4$. In this work, $H/W = 6$ is assessed since reflects some usual geometries of interest for the authors. $H/W = 10$ is also common practice and is recommended by DNV-RP-F108.[9]
In general, ISO 12135[8] presents more restrictive formulations and was therefore not discussed here (for example, only $0.45 \le a/W \le 0.70$ crack relative depths can be employed and SE(T) geometry is not supported).

5 ANALYSIS MATRIX

In this context, the analysis matrix for the 3D FE models included C(T), SE(B) and clamped SE(T) specimens of varying a/W ratios and side-groove depths as presented by Table 1, leading to 176 simulated conditions. Plane strain and plane stress 2D models were also developed for all a/W ratios to serve as limiting references (additional 42 models), but were not included for objectiveness purposes.
In general, 3D models considered 1T standard geometry with $W = 2B$, B = 25.4 mm (1 inch) and the remaining features following Figure 1, leading to W = 50.8 mm for example. For selected geometries (a/W = 0.2 and 0.5), 1/2T (B = 12.7 mm and $W = 4B$) and 2T (B = 50.8 mm and $W = B$) geometries were also studied keeping all other planar dimensions unchanged. This approach covered the recommendations of ASTM E1820[7] in terms of width-to-thickness ratios ($1 \le W/B \le 4$ for SE(B) and $2 \le W/B \le 4$ for C(T) specimens).
The total side-groove depths ($2r$ – Figure 1d) are based on the total thickness (B) of each specimen. For example, a 1T 10% side-grooved SE(B) specimen present r = 1.27 mm in each side, which means 2.54 mm in total (10% of B). The side-groove angle was for all models θ = 45º and is in accordance with current standards.

ISSN 1516-392X

Table 1. Selected geometries under investigation

Fracture specimens	C(T), SE(B), SE(T)						
Side-groove depths	0%, 5%, 10%, 20%						
a/W	**0.1**	**0.2**	**0.3**	**0.4**	**0.5**	**0.6**	**0.7**
1/2T		X			X		
1T	X	X	X	X	X	X	X
2T		X			X		

6 NUMERICAL PROCEDURES

Figure 4a illustrates the finite element model built for a/W = 0.5 considering C(T) geometry. All other crack models have very similar features. A conventional mesh configuration having a focused ring of elements surrounding the crack front is used with a small key-hole at the crack-tip; the radius of the key-hole, ρ_0, is 2.5μm (0.0025mm). Symmetry conditions permit modeling of only one-quarter of the specimens with appropriate constraints imposed on the remaining ligament and other symmetry planes. The quarter-symmetric models have 30 layers parallel to thickness including approximately 125000 8-node, 3D tri-linear hexahedric elements (~ 135600 nodes). The finite elements near the free surface are approximately 0.065 mm thick to better describe the discontinuity represented by the side-grooves. All finite element models are loaded by displacement increments to enhance numerical convergence.

An specific mesh generator was developed by the authors using MatLab platform in order to create the focused ring of elements near the crack tip (Figure 4a) combined to the desired geometry for the side-grooves. In Figure 4b one can see some developed meshes including 0%, 5%, 10% and 20% side-grooves in a C(T) specimen. A minimum of 8 elements describing the side-grooves was enforced (for the cases of 5% s.g.) looking for a good geometrical agreement to real samples. Deeper side-grooves incorporate more than 15 elements.

All models were processed in one step using the research code WARP3D v17.4[22] under small displacements and small-strain configuration. The material constitutive model is linear-elastic and was based on typical stress-strain data obtained from tensile tests of an API 5L X80 steel (E = 206 GPa and ν = 0.3).

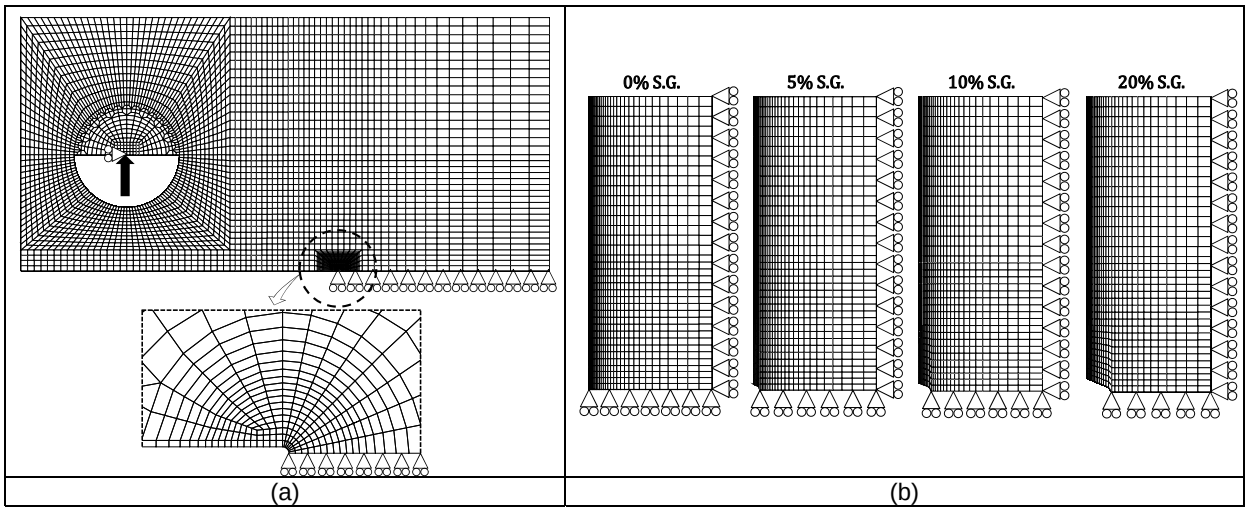

Figure 4. (a) Quarter-symmetric finite element model used for a C(T) specimens with a/W = 0.5. All other models present very similar features. (b) Different side-groove depths.

ISSN 1516-392X

7 RESULTS

7.1 Deviations on Crack Size Prediction Using Available Solutions

The developed FE models provided the evolution of load (P) *vs.* CMOD (V), leading to the expected compliance C for each geometry and material properties (E and ν). The effective thickness (B_{eff}) could be computed using Equation 3 and the normalized compliance (μ) using Equations 2 and 6 depending on the geometry considered. Crack size estimation formulae from ASTM (Equations 1, 4, 5 and 7) were then applied leading to the predicted a/W ratio (denoted here $a/W_{(ASTM)}$). Since the crack relative depth of each model is very well known, it can be used as a reference (and is denoted here $a/W_{(FEM)}$). Figure 5 presents the deviations found using ASTM solutions to predict model's a/W ratio using unloading compliance. Only errors regarding 1T geometries (the lower errors found) are presented here.
Figures 5a and 5b indicates that available solutions for C(T) specimens presented errors smaller than 2% only for $a/W \geq 0.5$. For shallow cracks ($a/W \leq 0.2$) deviations are over 7%. The existence of side-grooves and its depth presented small effects on assessed errors. Considering SE(B) specimens, Figure 5c shows that deviations were larger than 5% for $a/W = 0.1$, but rapidly decreases for 1% for $a/W \geq 0.2$. The same trend was observed for clamped SE(T) specimens (Figure 5d). A larger effect of side-grooves on errors was observed for SE(B) and SE(T) geometries. Particularly for shallow-cracked samples, these errors are considered inappropriate. For 1/2T and 2T geometries errors were even greater and this context motivated this investigation.

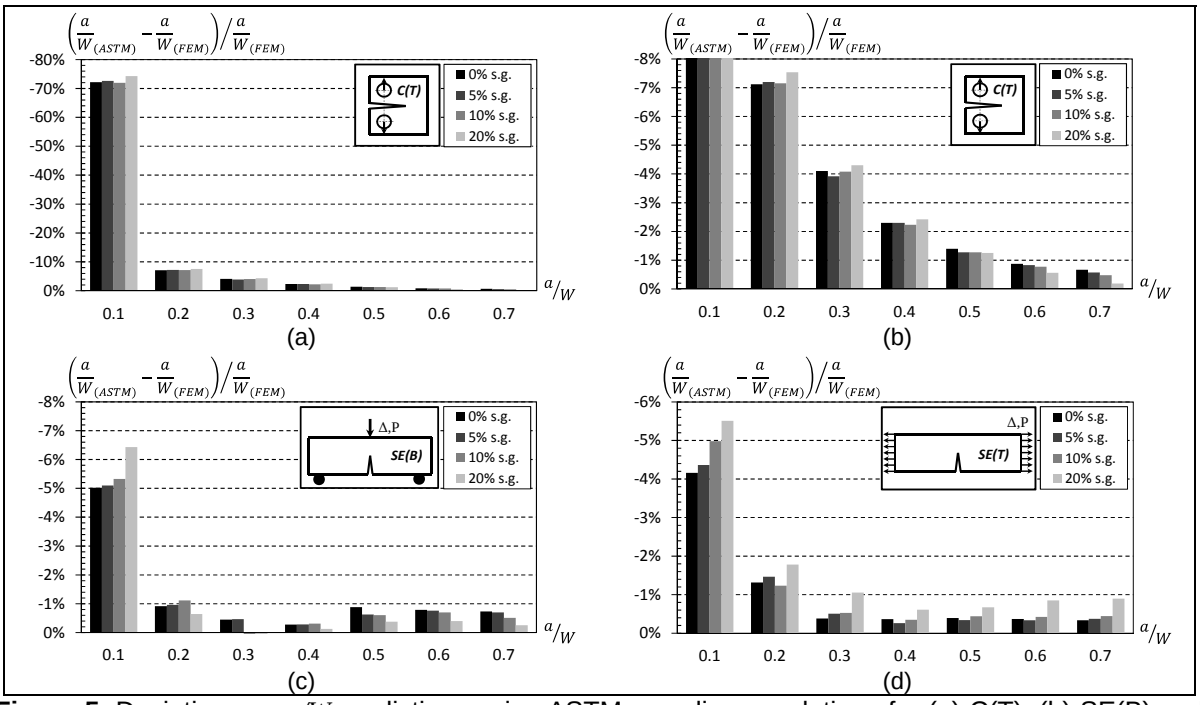

Figure 5. Deviations on a/W predictions using ASTM compliance solutions for (a) C(T), (b) SE(B) and (d) clamped SE(T) specimens.

7.2 Validation of Standardized Effective Thickness

After the errors provided by available standards and references were verified, an exploratory evaluation was conducted to validate effective thicknesses suggested by ASTM (Equation 3). For each FE model containing side-grooves, was determined the

ISSN 1516-392X

B_{eff} that could reproduce the ratio (*stiffness/B*) of the same geometry without side-grooves. Figures 6a to 6c compare the FE results to the B_{eff} predictions of Equation 3, respectively for C(T), SE(B) and clamped SE(T) geometries. Since the ordinate scales range from 0.92 to 1.02, it can be realized that deviations are quite small. The quantitative evaluation of the errors revealed that, for the 1T geometries presented here, Equation 3 can be used with errors less than ~ 2.5% for C(T), ~ 2.6% for SE(B), and ~ 1.5% for SE(T). It is worth mentioning that these error levels were verified in all cases for a/W = 0.7. For crack relative depths between 0.1 ≤ a/W ≤ 0.5 errors were under ~ 1.0% for every evaluated 1T geometry. Consequently, Equation (3) was adopted for all compliance proposals that follow.

7.3 Compliance Solutions Including Side-Grooves and 3D Effects

Based on FE results and using Equation 3 for B_{eff}, the normalized dimensionless compliance (μ) could be determined for each geometry, crack depth and side-grooves dimensions. Equation 2 was employed for C(T) and SE(T) specimens, while Equation 6 for SE(B). Figure 7a presents the obtained results for all cases. It can be noted that clamped SE(T) reveals larger values of μ if compared to C(T) and SE(B) geometries. However, the most relevant fact here is that results for all side-groove depths were included in Figure 7a, but markers are practically coincident and cannot be distinguished (for example, for SE(T) specimen with a/W = 0.5, four triangular markers are almost coincident, representing 0%, 5%, 10% and 20% side-grooves). Motivated by these results, Figures 7b to 7d present the best 5th order polynomial fit for the 28 available results considering each geometry. The proposed solutions predict a/W as a function of normalized elastic compliance (μ), independent on the side-grooves depth. In all cases, it was observed that the multiple correlation coefficient (R^2) almost reaches unity. It is important since guarantees that proposed formulations will include minimum errors on final computations.

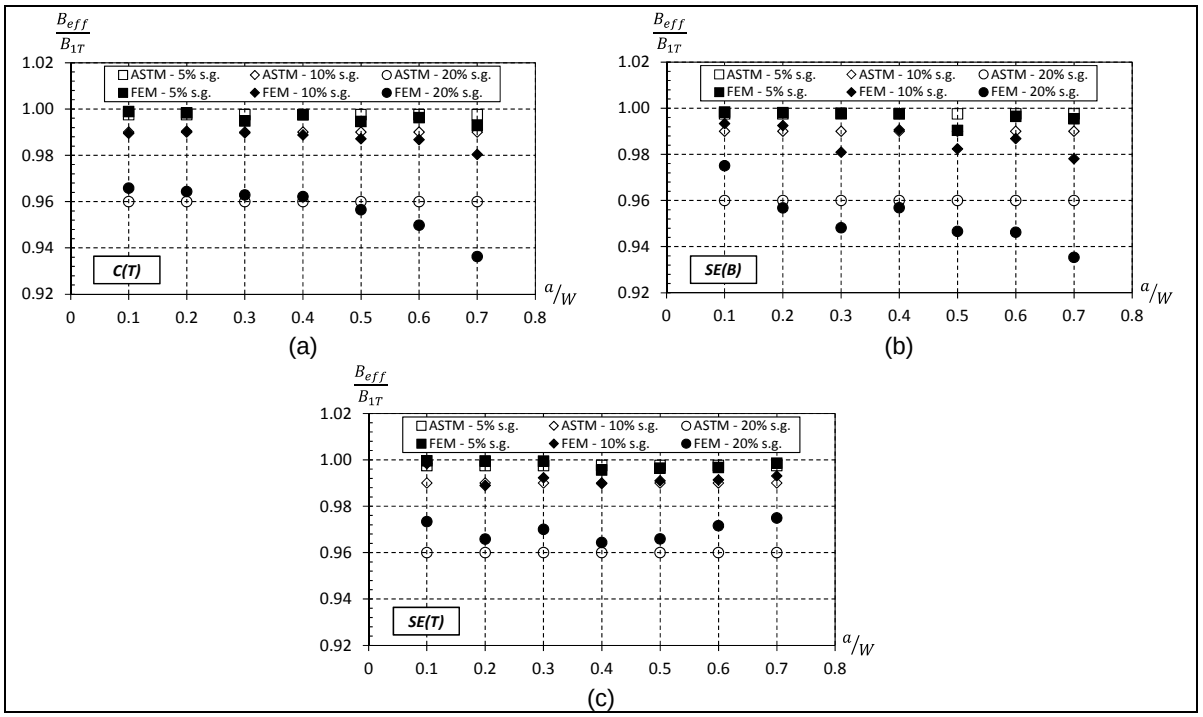

Figure 6. Deviations between B_{eff} predicted by ASTM using Equation 3 and from FEM computations. Results evaluated for 1T geometries.

ISSN 1516-392X

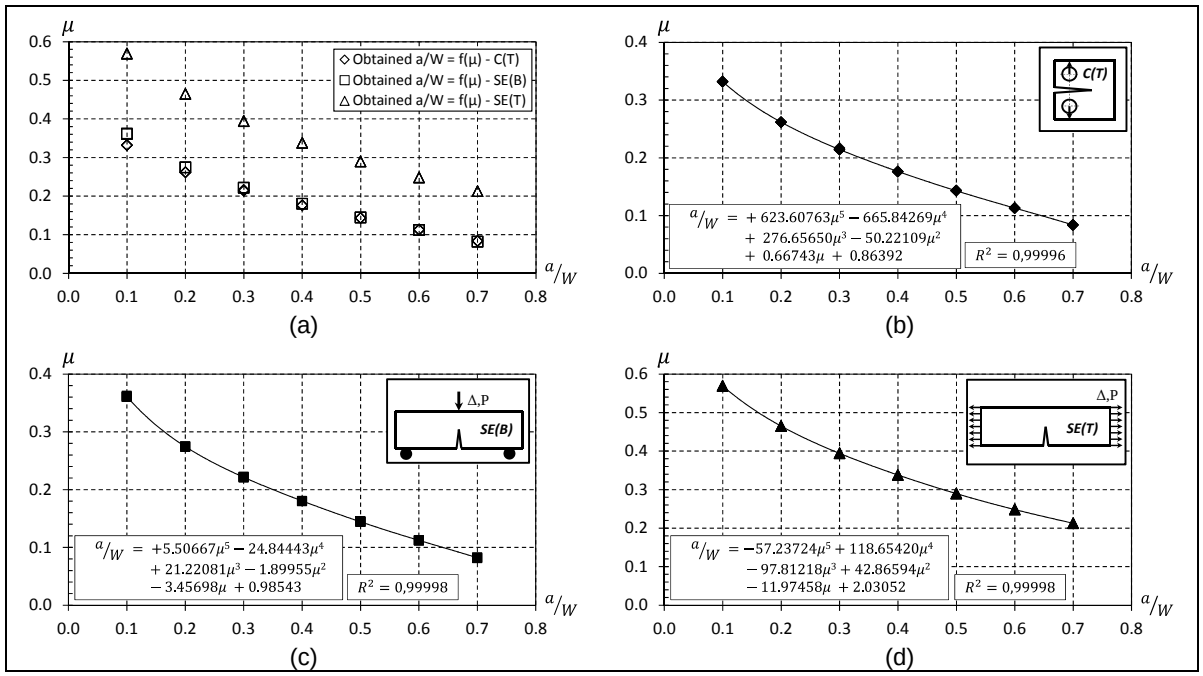

Figure 7. Normalized dimensionless compliance (μ). (a) All considered geometries, (b) C(T), (c) SE(B) and (d) clamped SE(T) with *H/W = 6*. All side-grooves depths are represented and markers are practically coincident.

7.4 Proposed Models for Crack Size Estimation

To organize the proposed formulations in a similar fashion when compared to ASTM standards, Equation 8 represents the general 5th order polynomial function to predict a/W from experimental compliance data. Table 2 provides the β coefficients that can be used in Equation 8 depending on the desired specimen.

$$\frac{a}{W} = \beta_0 + \beta_1\mu + \beta_2\mu^2 + \beta_3\mu^3 + \beta_4\mu^4 + \beta_5\mu^5 \tag{8}$$

Table 2. Fitting coefficients from fig. 7 applicable to Equation 8. Minimum achieved R^2 was 0.99996. Obtained from 1T, $W = 2B$ 3D FE models

Spec.	β_0	β_1	β_2	β_3	β_4	β_5
C(T)	0.86392	0.66743	-50.22109	276.65650	-665.84269	623.60763
SE(B)	0.98543	-3.45698	-1.89955	21.22081	-24.84443	5.50667
SE(T)	2.03052	-11.97458	42.86594	-97.81218	118.65420	-57.23724

In order to qualify the accuracy of proposed polynomial fittings for practical application, errors in a/W predictions were assessed. The FE models provided all geometrical features and the expected compliance (C) that should be obtained from real partial unloadings (considering R-curve testing) or hysteresis loops (considering FCG testing). Using B_{eff} from Equation 3 and μ from Equation 2 and 6, the proposed formulations of Equation 8 and Table 2 could be employed providing the expected a/W ratios. All side-groove depths were investigated and all results for 1T C(T), SE(B) and SE(T) geometries can be found respectively in Figures 8a, 8b and 8c. It can be realized that deviations in general do not overcome 0.4% and that side-groove effects could be well accommodated by the proposed formulae. The only geometries which presented larger errors were: i) SE(B) and SE(T) with a/W = 0.1 and 20% side-grooves, whose errors were ~ -0.8%; ii) C(T) with a/W = 0.3 and 20% side-grooves,

ISSN 1516-392X

whose error was ~ -1.5% (in this case, the deviation looks anomalous but no mistakes on models or data post-processing could be found). Therefore, results can be considered of high accuracy for crack-size estimation employing unloading compliance technique.

The effects of W/B ratio was also assessed in this investigation. The main motivation is that 2T ($W = B$) specimens present more volume of material ahead of the crack tip experiencing plane strain conditions if compared to 1T ($W = 2B$) and ½T ($W = 4B$) geometries. The opposite is true for ½T geometry, where relatively more material experiences plane stress conditions. Therefore, B_{eff} is influenced and deviations presented by Figure 6 are slightly increased for these geometries. Corrections for effective thickness could be developed, but were not implemented since deviations found were considered by the authors as acceptable. However, errors for selected conditions were assessed.

Figures 8d to 8f present the expected errors on crack-size estimation using the proposals of this work for ½T and 2T specimens containing cracks of a/W = 0.2 and a/W = 0.5. For C(T) specimens (Figure 8d) deviations are under ~ ±1%, for SE(B) specimens (Figure 8e) deviations are under ~ ±3% and for SE(T) specimens (Figure 8f) deviations are under ~ ±2%. In addition, it is worth noting that deviations for ½ T geometries are lower than for 2T geometries. This is relevant since C(T) specimens used for FCG testing usually lie between ½T and 1T.

The errors presented by Figures 8d to 8f are in agreement with the expected trends. In general, a/W ratios are overestimated by current proposals for ½T geometries, since these specimens are slightly more compliant. The opposite happens for 2T geometries, where underestimations are observed.

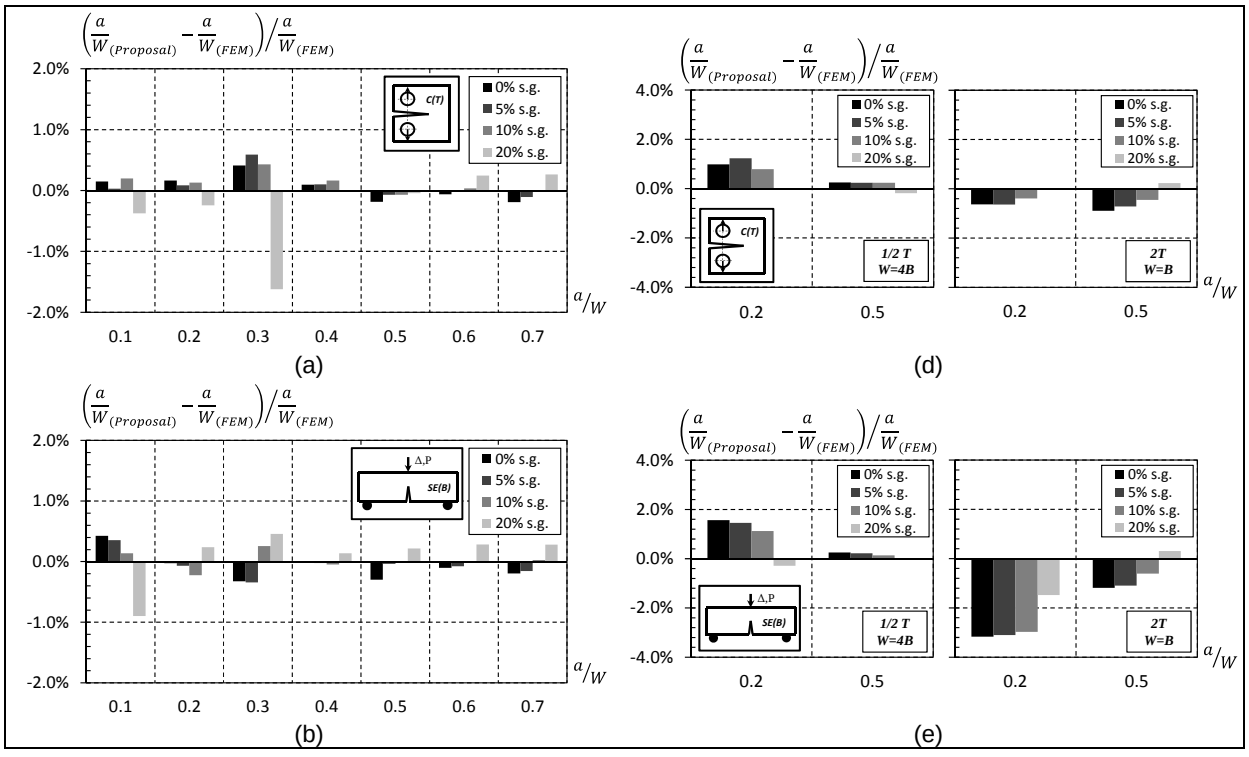

ISSN 1516-392X

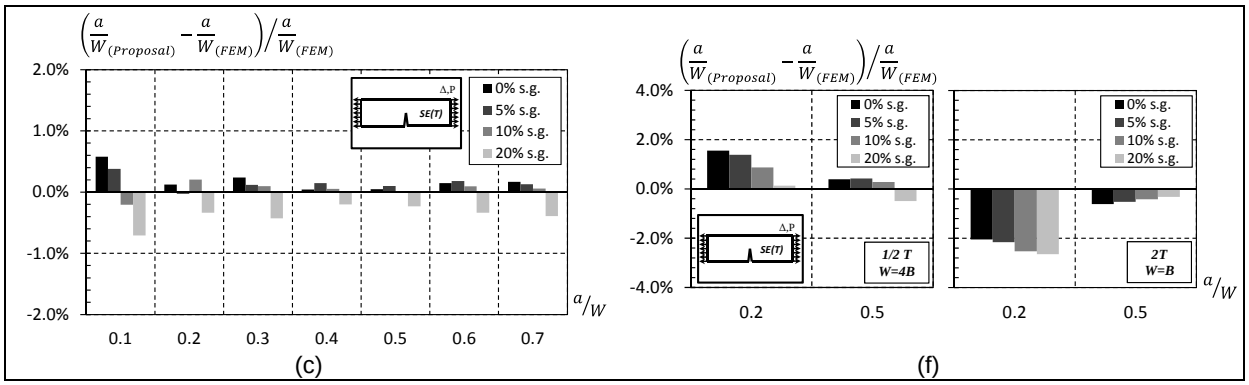

Figure 8. (a-c) Deviations when predicting *a/W* ratios for the developed 1T (*W* = *2B*) FE models using the proposed formulations of Equation 8 and Table 2. (d-f) Same results for ½T (*W* = *4B*) and 2T (*W* = *B*).

8 CONCLUDING REMARKS

From this work, the following central conclusions emerge:

- compliance solutions from standards and existing references presented deviations over 6% - 10%, particularly for side-grooved shallow-cracked samples;
- regarding effective thickness (B_{eff}), the errors of Equation 3 from ASTM were under ~ 1.0% for every 1T geometry between $0.1 \leq a/W \leq 0.5$. For deeper cracks ($0.5 < a/W \leq 0.7$), errors were under ~ 2.6% and Equation 3 was assumed accurate;
- fortunately, there was a minimum effect of side-grooves on μ and a single 5th order polynomial fit could agree to all 28 *a/W vs.* μ results for each geometry.
- all proposed formulae have $R^2 \geq 0.99996$ for 1T (*W* = *2B*) geometrical features;
- deviations on *a/W* prediction using the proposed models did not overcome 0.4 % even considering 20% side-grooves, indicating high accuracy for 1T geometries. If compared to standardized solutions, deviations were strongly reduced;
- the application of the proposed model to ½T (*W* = *4B*) and 2T (*W* = *B*) geometries revealed slightly larger deviations (deviations are under ~ ±1% for C(T), under ~ ±3% for SE(B) and under ~ ±2% for clamped SE(T)).

Combined to existing methodologies for R-curves and FCG testing, the proposed solutions increase accuracy in crack-size estimation for C(T), SE(B) and clamped SE(T) specimens incorporating 3D and side-groove effects. The more precise mechanical properties favor structural integrity activities and safety of applications.

Acknowledgment

This investigation was supported by FAPESP (Fundação de Amparo à Pesquisa do Estado de São Paulo) and by the Ignatian Educational Foundation (FEI, Brazil) through materials, laboratories and human resources.

REFERENCES

1 ANDERSON, T. L. **Fracture Mechanics: Fundamentals and Applications**, 3rd edition, New York, CRC Press, 2005, 640 p.

ISSN 1516-392X

2 AMERICAN PETROLEUM INSTITUTE. **API RP 579-1: Recommended Practice for Fitness-for-Service**, 2nd edition, 2007, 1126 p.
3 BRITISH STANDARDS INSTITUTION. **BS 7910:2005: Guide to methods for assessing the acceptability of flaws in metallic structures**, England, 2005, 306 p.
4 HARRISON, R.P.; LOOSEMORE, K.; MILNE, I.; DOWLING, A.R. **Assessment of the Integrity of Structures Containing Defects**, CEGB Report R/H/R6 – rev. 2, Central Electricity Generating Board, United Kingdom, 1980.
5 STRUCTURAL INTEGRITY ASSESSMENT PROCEDURES FOR EUROPEAN INDUSTRY. SINTAP; Final Report, July, 1999.
6 DET NORSKE VERITAS. **DNV-OS-F101: Submarine Pipeline Sys.**, Norway, 2012.
7 AMERICAN SOCIETY FOR TESTING AND MATERIALS. **ASTM E 1820: Standard Test Method for Measurement of Fracture Toughness**, Philadelphia, 2011.
8 INTERNATIONAL ORGANIZATION FOR STANDARDIZATION. **ISO 12135: Metallic materials - Unified method of test for the determination of quasistatic fracture toughness**, Switzerland, 2002.
9 DET NORSKE VERITAS (DNV). **DNV-RP-F108: Fracture Control for Pipeline Installation Methods Introducing Plastic Strain**, Norway, 2012.
10 MOREIRA, F. C., DONATO, G. H. B. **Estimation Procedures for J and CTOD Fracture Parameters Experimental Evaluation using Homogeneous and Mismatched Clamped SE(T) Specimens**, Pressure Vessel and Piping, 2010.
11 CRAVERO, S., RUGGIERI, C. **Correlation of Fracture Behavior in High Pressure Pipelines with Axial Flaws Using Constraint Designed Test Specimens - Part I: Plane-Strain Analyses**, Engineering Fracture Mechanics, Vol.72, 2005, p. 1344-1360.
12 CRAVERO, S. RUGGIERI, C. **Estimation Procedures of J-Resistance Curves for SE(T) Fracture Specimens Using Unloading Compliance,** Engineering Fracture Mechanics, Vol.74, 2007, p. 2735-2757.
13 AMERICAN SOCIETY FOR TESTING AND MATERIALS. **ASTM E 647: Standard Test Method for Measurement of Fatigue Crack Growth Rates**, Philadelphia, 2013.
14 SHEN, G., TYSON, W. R., GIANETTO, J. A., PARK, D. **Effect of Side Grooves on Compliance, J-integral and Constraint of a Clamped SE(T) Specimen**, PVP, 2010.
15 SHEN, G., TYSON, W. R., GIANETTO, J. A. **CMOD Compliance of BxB Single Edge Bend Specimens**, Pressure Vessel and Piping, 2012.
16 SAXENA, A. **Nonlinear Fracture Mechanics for Engineers**, CRC Press, 1998.
17 SURESH, S. **Fatigue of Materials**, Cambridge University Press, UK, 1998.
18 TADA, H., PARIS, P. C., IRWIN, G. R. **The Stress Analysis of Cracks Handbook**, Del Research Corporation, Hellertown, PA, 1973.
19 JOYCE, J. A. **J-R Curve Testing of Short Crack Bend Specimens using Unloading Compliance**, Fract. Mech. 22nd Symposium, ASTM STP1131 (V. I), 1992, pp. 904-926.
20 WU, S. **Crack Length Calculation Formula for Three Point Bend Specimens**, International Journal of Fracture, 1984, p. 33-38.
21 WANG, E., ZHOU, W. **A Numerical Study on CMOD Compliance for Single-Edge Bending Specimens**, Pressure Vessel and Piping, 2012.
22 KOPPENHOEFER, K.; GULLERUD, A.; RUGGIERI, C.; DODDS, R.; HEALY, B. **WARP3D: Dynamic Nonlinear Analysis of Solids Using a Preconditioned Conjugate Gradient Software Architecture**, Structural Research Series (SRS) 596. UILU-ENG-94-2017. University of Illinois at Urbana-Champaign, 1994.